https://doi.org/10.56801/MME1013

Study of Mechanical-Elastic Parameters of Reservoir Rocks with Respect to the Purpose of Permanent CO_2 Storage

Adam Lacman[1], Matěj Křístek[2], Patricie Karol[3], Martin Klempa[4]

[1,2,3,4]*Department of Geological Engineering, Faculty of Mining and Geology, VSB – Technical University of Ostrava, Ostrava, Czechia*

Received: 06-09-2023
Accepted: 13-09-2023

Abstract: CO_2 emissions are considered to be partly responsible for climate change. One of the available methods to reduce CO_2 emissions is its storage in favorable rock structures, such as mined hydrocarbon deposits. Natural hermeticity is guaranteed with this reservoir structure. An increase in pressure conditions in the deposit, induced by long-term CO_2 storage, can lead to the splitting of exposed rocks. It is therefore necessary to carry out geomechanical tests on available drill core samples. The presented article presents the results of laboratory research aimed at determining the mechanical-elastic parameters of reservoir rocks of a hydrocarbon deposit using non-destructive testing. The advantage of this method is the possibility of testing the given samples before and after exposure to CO_2. The laboratory research carried out revealed significant differences in the measured mechanical-elastic parameters of the tested samples. Taking into account that samples of the consistent reservoir structure of the same deposit were tested, the necessity of detailed testing of geomechanical parameters arises. It was interpreted that the differences in mechanical-elastic parameters found by the research may be caused by differences in the lithological composition (for these purposes, XRD powder diffraction was implemented), or by mechanical disturbance given, for example, by fracture predisposed by structural-tectonic processes. Different humidity can also have an effect, or degree of saturation of the tested samples.

Keywords: elastic waves, mechanical-elastic parameters, geomechanical testing, CO_2 storage, reservoir carbonate rock.

1. Introduction

The production of carbon dioxide is constantly increasing due to the burning of fossil fuels needed to produce electricity and heat, as well as due to the increase in industry and transport. Half of this produced carbon dioxide is consumed by plants, part dissolves in the oceans, but the rest of the gas escapes into the atmosphere, where the greenhouse effect and global warming of our planet are increasing. The purpose of building underground reservoirs in extracted oil and natural gas deposits is to permanently store CO_2 in order to reduce the concentration of CO_2 in the atmosphere.

The subject of the research is non-destructive geomechanical testing of rock samples from the undermined oil and gas deposit Žarošice, which is located in the region of southeastern Moravia (Figure 1). The location appears to be a suitable place for long-term storage of carbon dioxide emission gas. Drill core samples were obtained from the deposit, on which geomechanical testing was carried out. As part of the research, a combination of several testing methods is appropriate with the aim of comprehensive knowledge of the deposit and the creation of a model for CO_2 injection. One method is the non-destructive measurement of drill cores of known length, diameter, weight, and volume. In this way, the geomechanical parameters of individual rock samples, which are the focus of this article, can be obtained.

The injection of CO_2 into carbonates affects the petrophysical, mechanical-elastic properties of rocks, which require a quantitative analysis aimed at determining the storage capacity for CO_2. The effort is to ensure the safety and long-term functioning of the underground reservoir. [1, 2].

Figure. 1. Location of the oil and gas deposit Žarošice [3]

1.1. Effect of injected CO_2 on changes in geological structures

Carbon dioxide is injected into the underground reservoir in the form of a supercritical liquid. Under the influence of pressure and temperature, it dissolves in the water contained in the pores of the rock and carbonic acid is formed, which contributes to the dissolution of minerals. [4] During the secondary precipitation of minerals, changes in the pore space subsequently occur, which can affect the flow transport paths as well as the mechanical properties of the rock [5-7].

The brine saturated with CO_2 reacts with anhydrite, calcite, and dolomite. Acidification of the system causes changes in the pore structure. These can be manifested by the expansion of existing pores, the overall increase or decrease of micropores, and the creation of new flow channels. An increase in permeability is usually associated with the dissolution of minerals, while a decrease in permeability is attributed to the secondary precipitation of minerals and the blocking of pore openings [8, 9].

When CO_2 is injected into the rock, the pore pressure increases, which reduces the shear strength. Increased pore pressure can cause reactivation of existing or new fractures, geomechanical deformations or subsidence of overlying layers, and compaction of rocks present in the deposit [10].

1.2. Characteristics of the Žarošice deposit

From a geological point of view, the Žarošice oil and gas deposit is located in the SE region of the Bohemian Massif. Potentially usable storage for CO_2 consists of Jurassic Vranovician carbonate rocks and there are dolomites with limestones and sandstones. Figure 2 shows a geological section of the site, which consists of an oil field with a gas cap and an active aquifer [11].

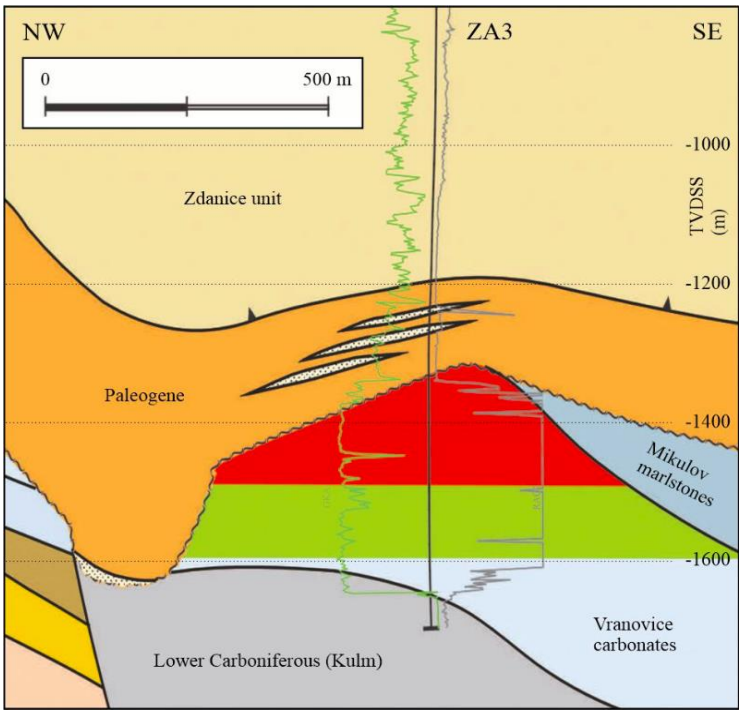

Figure. 2. Geological cross section through the structure of interest [12]

The rocks in this lithostratigraphic unit are of different types, from light-gray to silty-gray limestones to organodetritic-silty limestones, partly dolomitized, often even dolomites. These limestones are variably to strongly silicified with positions of lenses and dark brown and dark gray cherts with a typical wormy texture [13]. The Vranovick limestones are formed by a sedimentary series of biomicritic detritus and silt, which was flushed from the shelf carbonate plateau in the west (stratigraphic classification=Oxford; base of the Lower Kimmeridgian). The Vranovick limestones were gradually formed from the underlying Nikolčice layers. The thickness of the underlying Nikolčice layers decreases to the east towards the deeper parts of the basin. This was proven during the exploration of the newly discovered Žarošice hydrocarbon field in Central Moravia. The Vranovick limestones represent a very good reservoir for the occurrence of oil and natural gas. The intensity of limestone dolomitization decreases on the southeastern edge of the Bohemian Massif, under the Carpathian foreland and the mantle of the Western Carpathians. From the point of view of the accumulation of natural hydrocarbons, these limestones have been found to have good collector properties in their lower part in the Uhřice area. This claim was proven in 2001 by the discovery of the Žarošice oil deposit, where the oil is accumulated precisely in these so-called cavernous dolomites [14].

1.3. Geomechanical testing

The subject of the research is geomechanical testing of rock samples from the undermined oil and gas deposit Žarošice, which is located in the region of southeastern Moravia. The location appears to be a suitable place for long-term storage of carbon dioxide

emission gas due to the hydrodynamic closure of the horizon. In addition, CO_2 can be injected into the deposit to increase oil and gas recovery. [15] Drill core samples were obtained from the deposit and geomechanical testing was carried out on them. The rock samples were modified to achieve a regular cylindrical shape. As part of the research, a combination of several testing methods is appropriate with the aim of comprehensive knowledge of the deposit and the creation of a model for CO_2 injection. A total of 6 samples, taken from four wells, were tested. The wells are designated with the working names BH1 to BH4.

1.4. Non-destructive testing of mechanical-elastic properties

The mechanical-elastic properties were determined non-destructively using the UKS-14 measuring device from Geotron-Elektronik (Figure 3). This mobile device consists of an ultrasound generator producing impulses with a frequency of 20-350 kHz. The tested samples are fixed in the respective mechanisms, where one base of the cylinder-shaped sample is fixed on the so-called exciter, which emits ultrasonic waves, and the other base is fixed on the so-called sensor, which receives the excited ultrasonic waves. The tested sample must always be properly fixed so that it does not rotate and at the same time does not touch any edges of the measuring apparatus.

The speed of propagation of ultrasonic waves is recorded by the measuring apparatus, while this speed depends on the physical-mechanical characteristics of the tested sample. The velocity of propagation of longitudinal waves (vP), transverse waves (vS), surface waves (vR) and plate waves (vD) is recorded. Mechanical-elastic properties are subsequently determined from the speed of propagation of longitudinal and transverse waves and the volumetric weight of the tested sample, dealing with the elasticity of the tested samples of injection mixtures. (UKS-14 manual)

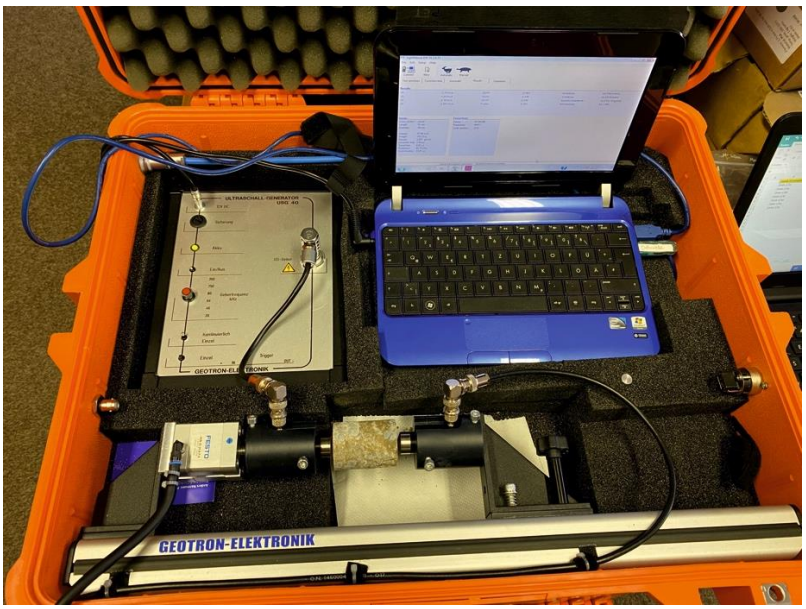

Figure. 3. UKS-14 measuring equipment from Geotron-Elektronik

Flexibility can be understood as the ability of a material to regain its original shape after the load is relieved. The modulus of elasticity can be defined - in the case of standard destructive tests - as the ratio of the stress and the deformation caused by it. The modulus of elasticity evaluated from destructive tests is called as static section modulus of elasticity. If the modulus of elasticity is evaluated on the basis of non-destructive tests, it is referred to as the dynamic tangent modulus of elasticity. It is often indicative that the dynamic modulus of elasticity reaches approximately 20 % higher values than the static modulus of elasticity.

As part of the research, the following mechanical-elastic properties were evaluated: Poisson's number, Young's dynamic modulus of elasticity, dynamic modulus of elasticity in shear, and dynamic modulus of bulk elasticity.

Poisson's number ν (2) means the ratio of transverse strain to longitudinal strain.

Young's dynamic modulus of elasticity E [Pa] is defined as the ratio of unidirectional stress and the deformation induced by it in this direction.

The dynamic shear modulus of elasticity G [Pa] can be understood as a material property describing the ratio between the shear stress and the deformation caused by it. There is a mutual relationship between Poisson's number μ, modulus of elasticity E and shear modulus of elasticity G, expressed by the following equation (1):

$$G = \frac{E}{2 \cdot (1+\mu)} \quad (1),$$

where: G = shear modulus of elasticity [Pa],
E = Young's modulus of elasticity [Pa]
μ = Poisson's number [16].

The dynamic modulus of volume elasticity K [Pa] is defined as the inverse value of volume compressibility, indicating the change in volume relative to the change in pressure. There is a relationship between Young's modulus E, Poisson's number, and bulk modulus of elasticity K, expressed by the following equation (2):

$$K = \frac{E}{3 \cdot (1-2 \cdot \mu)} \quad (2),$$

where: K = bulk modulus of elasticity [Pa],
E = Young's modulus of elasticity [Pa],
μ = Poisson's number [16].

In three-dimensional solid materials [17, 18], the following relations (3, 4, 5) apply between the propagation velocities of longitudinal and thus transverse waves and elastic-mechanical parameters:

$$V_P = \sqrt{\frac{K + \frac{4}{3} \cdot G}{\rho}} = \sqrt{\frac{E \cdot (1-\upsilon)}{\rho \cdot (1+\upsilon) \cdot (1-2 \cdot \upsilon)}} \quad (3),$$

$$V_S = \sqrt{\frac{G}{\rho}} \quad (4),$$

$$\frac{V_P}{V_S} = \sqrt{\left(\frac{1-\nu}{0{,}5-\upsilon}\right)} \quad (5),$$

where: V_P = velocity of longitudinal waves [$m \cdot s^{-1}$],

V_S = speed of transverse waves [$m \cdot s^{-1}$],

G = shear modulus of elasticity [Pa],

E = Young's modulus of elasticity [Pa],

K = bulk modulus of elasticity [Pa],

ν = Poisson's number [16].

1.5. Non-destructive testing of physical properties

From the spectrum of physical properties, porosity, permeability, pore and volume compressibility and Biott coefficient were determined.

Porosity represents all the spaces between rock grains that are not filled with solid matter. Pores include cavities and fissures. Hydrocarbon deposits are characterized by pores that are interconnected. We distinguish primary (syngenetic), which arose together with the rock, and secondary (epigenetic), which arose due to changes in the conditions in the rock (dissolution of rock components or volume change, for example during dehydration). [15] In their article, the authors Kassab and Weller [19] rank porosity among the most important factors affecting the speed of P-wave flow. Thus, the velocity of P-waves decreases with increasing porosity. Sharo and Al-Tawaha [20] also report that the P-wave propagation speed increases with volume and decreases with porosity.

Permeability allows a liquid or gas to pass through a rock environment through pores or along fractures [15].

According to Zimmerman [21], pore compressibility is of two types. Hall [22] determined the formation compaction coefficient (C_{pc}) and effective pore compressibility (C_{pp}), which indicate the dependence of the pore volume on changes in confining pressure or liquid pressure in the pores. The first deals with changes in pore volume as a function of increasing pore pressure in rocks according to the following relationship (6). The second follows the changes in the pore volume depending on the decreasing pore pressure at the maximum constant stress according to relation (7):

$$C_{pc} = \frac{-1}{V_p^i}\left(\frac{\partial V_p}{\partial P_c}\right)_{P_p} \quad (6),$$

$$C_{pp} = \frac{1}{V_p^i}\left(\frac{\partial V_p}{\partial P_p}\right)_{P_c} \quad (7),$$

where: V_p = pore volume,

P_p = pore pressure,

P_c = confining pressure.

From the equation below (8), it can be seen that C_{pc} can be converted to C_{pp} using Biot's coefficient ($\propto$). (Biot, 1941)

$$\propto_p = \frac{C_{pp}}{C_{pc}} \quad (8),$$

where $\propto_p$ can be determined based on a comparison of the size of the volume compressibility of the pores and the changes in the lateral (confining) and pore pressure.

Rock bulk compressibility C_B (Rock bulk compressibility) is defined as the proportion of change in rock volume per unit pressure change [23] according to the following relationship:

$$C_B = -\frac{1}{V_B}\left(\frac{\partial V_B}{\partial p}\right)_T \quad (9),$$

where: C_B = rock - bulk compressibility,

V_B = bulk volume.

Biot's coefficient is defined as the ratio of the liquid volume of the material to the change in the volume of the solid when the pore pressure changes according to the relationship [24]:

$$\alpha = 1 - \left(\frac{K}{K_s}\right) \quad (10),$$

where: K = bulk modulus,
K_s = bulk modulus of the solid component.

1.6. Measurement results

The results of the above-mentioned geomechanical testing are shown in Table 1. For better graphic clarity, the values in the individual columns of the graphic table are highlighted, according to this scheme:

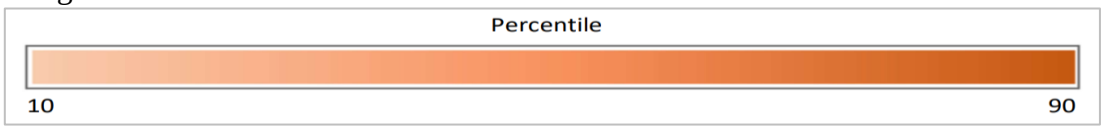

Table 1. Results of measured values of mechanical-elastic, petrophysical and mechanical properties of rock samples

Sample ID	Por. (%)	Per. (mD)	Density ($g \cdot cm^{-3}$)	v_P ($km \cdot s^{-1}$)	v_S ($km \cdot s^{-1}$)	ν_dyn (-)	E_dyn (GPa)	G_dyn (GPa)	K_dyn (GPa)	Unc. comp. str. (MPa)	Pore compr. V_{pc} (MPa^{-1})	Bulk compr. C_{bc} (MPa^{-1})	Biot coeff. (-)
BH1	1,41	0,17	2,72	4,748	2,587	0,29	46,98	18,23	37,11	55,23	1,52E-03	3,45E-05	0,637
BH2/1	2,50	21,56	2,57	3,584	1,739	0,35	20,93	7,77	22,66		6,99E-03	2,17E-04	0,942
BH/2	3,77	12,93	2,49	2,838	1,236	0,38	10,50	3,80	14,96	3,09	1,12E-03	5,53E-05	0,773
BH3/1	2,79	1,22	2,55	4,516	2,224	0,34	33,76	12,60	35,15		2,16E-03	7,55E-05	0,834
BH3/2	1,61	1,50	2,69	4,830	1,638	0,44	20,72	7,22	53,14	61,98	4,81E-03	9,75E-05	0,871
BH4	3,63	0,58	2,73	4,639	2,135	0,37	33,99	12,44	42,17		2,62E-03	1,11E-04	0,887

It can be seen from Table 1 that, although samples from the same deposit and the same reservoir structure were tested, relatively significant differences in mechanical-elastic parameters are recorded. Graphical representation of dynamic modulus of elasticity (E, G, K) and speed of propagation of elastic waves, respectively. Poisson's numbers can be seen in Figure 4.

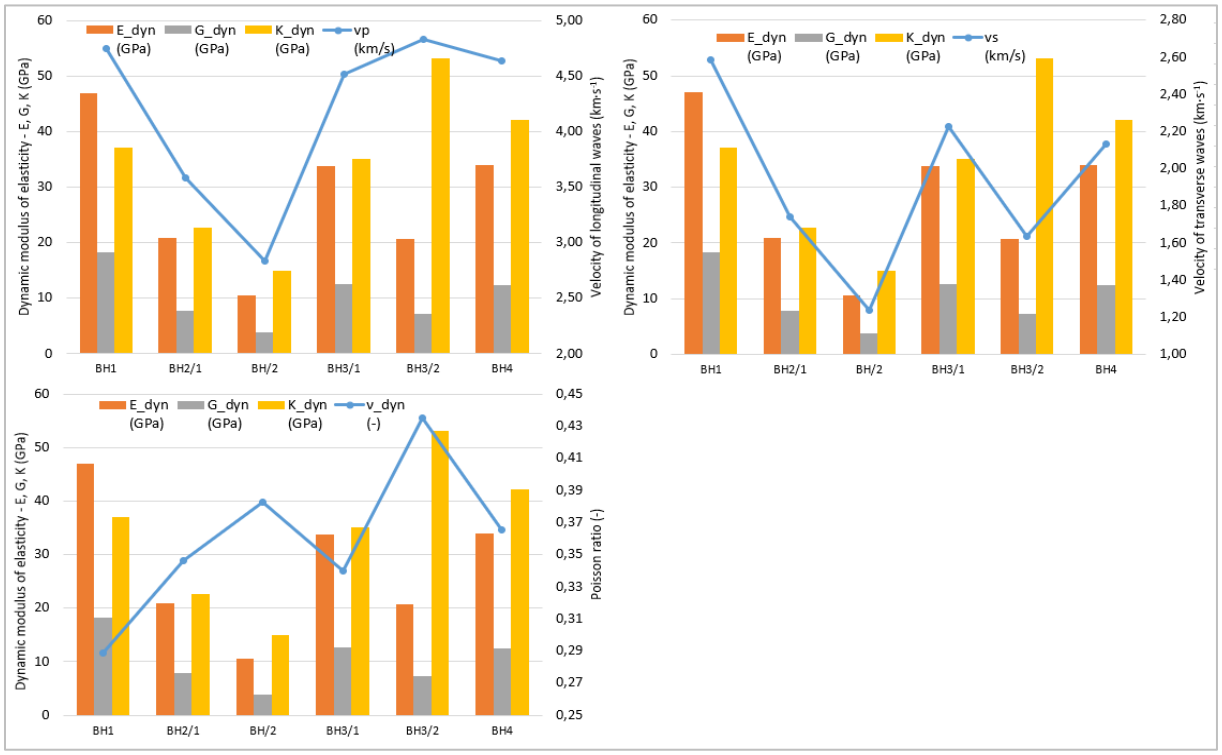

Figure. 4. Graphical representation of dynamic modulus of elasticity (E, G, K) and speed of propagation of elastic waves, respectively Poisson numbers

The dependence (linear regression) between the speed of longitudinal and transverse waves can be seen in Figure 5.

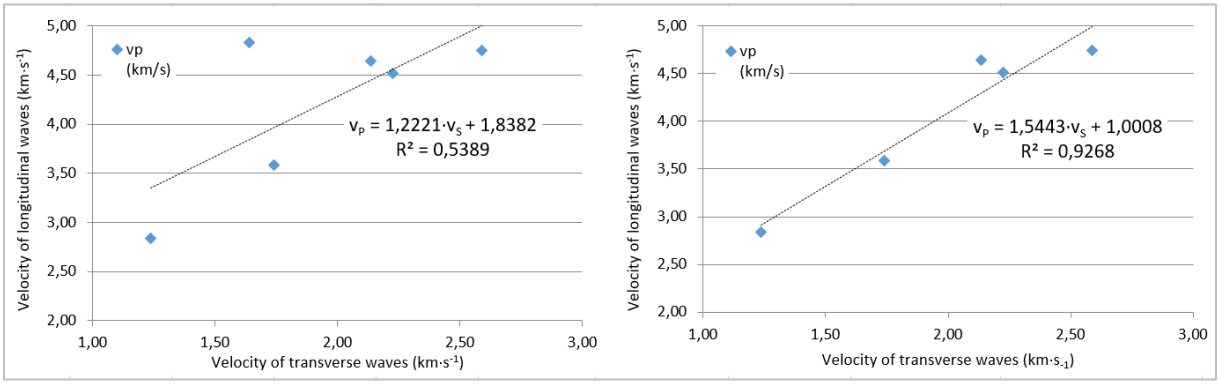

Figure. 5. Dependence (linear regression) between the speed of longitudinal and transverse waves

The different speed of elastic waves and the different values of mechanical-elastic parameters determined from it can be caused by the following factors:

1) Different mineralogical composition;
2) Different strength bonds (mechanical disruption of rocks, induced mainly by structural-tectonic processes);
3) Different porosity;
4) Different degree of saturation;
5) Anisotropy of rock samples.

1.7. A factor of different mineralogical composition

The different speeds of propagation of elastic waves can be caused by the different mineralogical compositions. Powder PXRD (powder X-Ray diffraction) was implemented to assess whether the tested carbonate rocks differ from each other in mineralogical composition. PXRD was performed on four rock samples taken from four wells (BH1 to BH4). The results are shown in Figure 6.

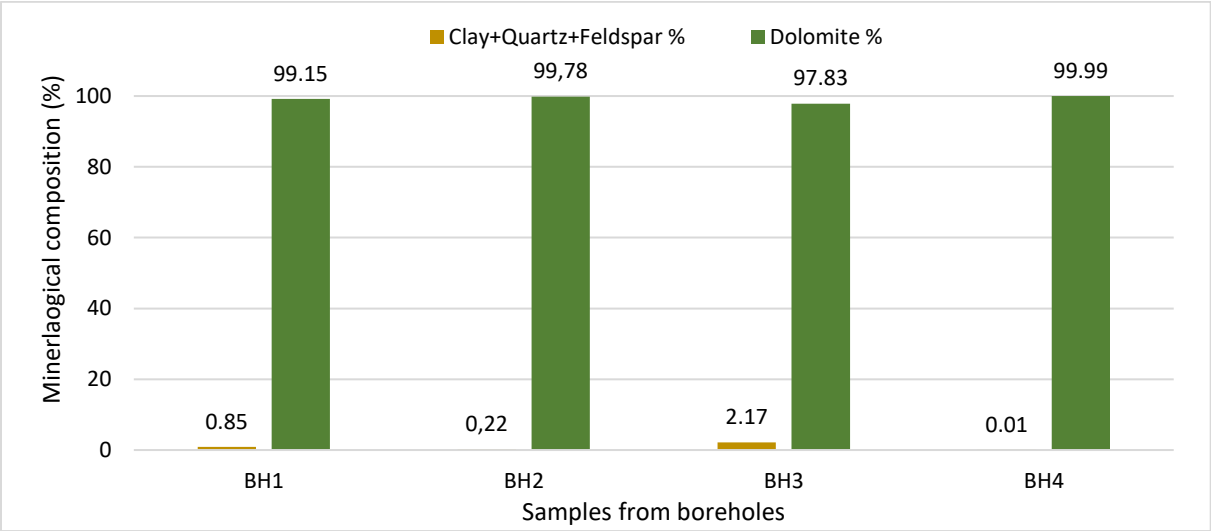

Figure. 6. Mineralogical composition of rock samples taken from boreholes BH1 to BH4

It can be seen from Figure 6 that the tested samples do not differ from each other in mineralogical composition. These are rocks practically almost exclusively formed by the mineral dolomite.

A different mineralogical composition was not demonstrated. It is therefore not a factor causing the different propagation speed of elastic waves.

1.8. Factor of differential strength bond

The different speeds of propagation of elastic waves can be caused by different strength bonds. The presence of discontinuities created mainly during structural-tectonic processes or any other weakening of strength bonds causes a reduction in the propagation speed of elastic waves. Three of the six tested samples were subjected to a destructive mechanical test to determine the strength of simple compression. The determination of the dependence (linear regression) between the simple compressive strength (UCS) and the velocity of transverse waves (V_S), the velocity of longitudinal waves (V_P), the dynamic modulus of elasticity (E_dyn) and the dynamic modulus of elasticity in shear (G_dyn) can be seen from Figure 7.

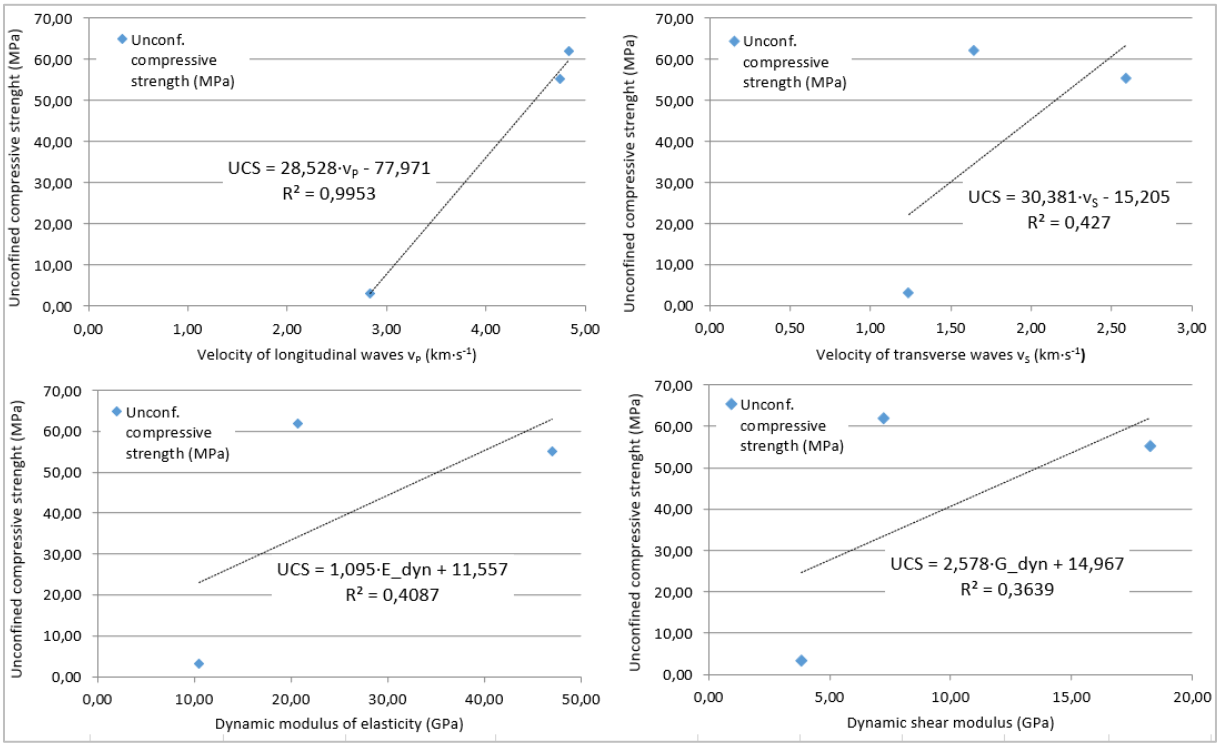

Figure. 7. Dependence (linear regression) between unconfined compressive strength (UCS) and velocity of transverse waves (V_S), velocity of longitudinal waves (V_P), dynamic modulus of elasticity (E_dyn) and dynamic modulus of elasticity in shear (G_dyn)

It can be seen from Figure 7 that the assumption of increasing propagation speeds of elastic waves and increasing values of dynamic modulus of elasticity with increasing values of strength in simple compression was generally fulfilled. A high R^2 reliability value is achieved in the dependence of linear regression of unconfined compressive strength (UCS) and velocity of transverse waves (V_S). On the contrary, it was found that a low R^2 reliability value is achieved in the linear regression dependence of longitudinal wave propagation speed (V_P) and unconfined compressive strength (UCS), which is likely to be explained by the particle arrangement of the tested samples through which the waves propagate. However, it is understandable that the degree of dependence between the monitored parameters cannot be reliably assessed from the three available data.

Different strength bonds have been demonstrated. On the basis of the obtained data, it can be concluded that the factor of different strength bonds affects the propagation speed of elastic waves, and therefore also the elastic-mechanical parameters. Dependence (linear regression) between unconfined compressive strength (UCS) and porosity (Por), resp. permeability (Per) can be seen from Figure 8.

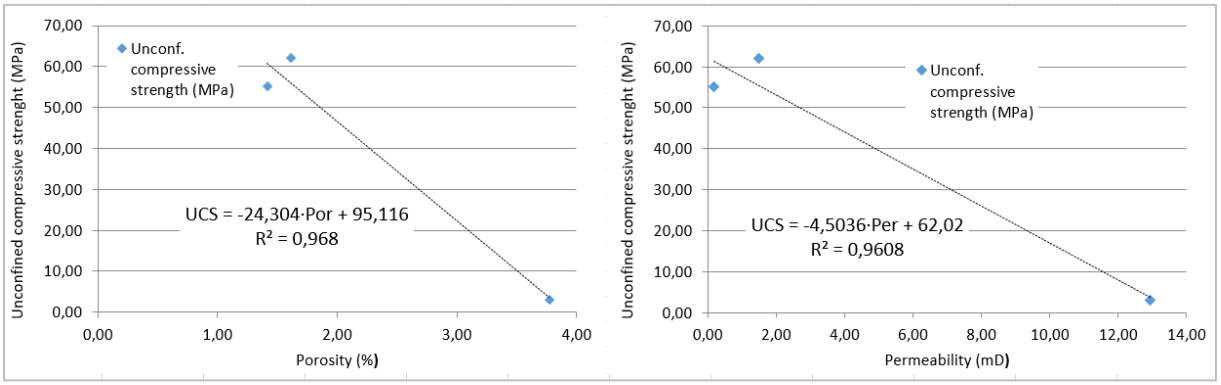

Figure. 8. Dependence (linear regression) between unconfined compressive strength (UCS) and porosity (Por), resp. permeability (Per)

It can be seen from Figure 8 that there is a linear regression relationship between the unconfined compressive strength and both porosity and permeability, with a high R^2 reliability value.

1.9. Differential porosity factor

The different propagation speeds of elastic waves can be caused by different porosity. Considering that rock samples of practically identical mineralogical composition were tested, it can therefore be assumed that the volumetric weight of the samples decreases with increasing porosity. In general, the higher the rock density, the lower the porosity and the higher the propagation speed of Vp waves. [25-28] The dependence (linear regression) between bulk density (Db) and porosity (Por) can be seen in Figure 9.

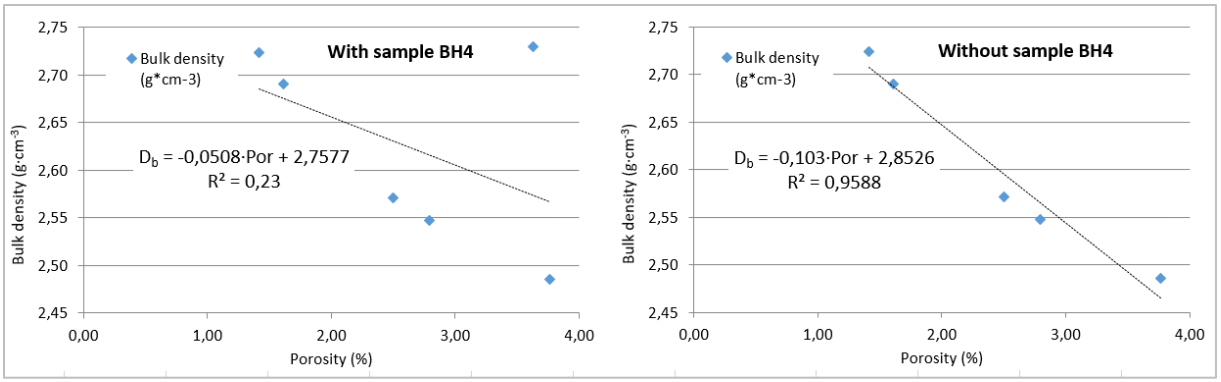

Figure. 9. Dependence (linear regression) between bulk density (Db) and porosity (Por)

It can be seen in Figure 9 that the assumption of increasing bulk density with decreasing porosity was generally confirmed. A high R^2 reliability value is achieved when the BH4 sample is not calculated. According to PXRD, the BH4 sample should not show a different mineralogical composition than the other samples. Therefore, we do not know why this sample violates the high confidence level of the linear regression. Further dependency evaluations performed below, therefore, do not compute with this sample.

The dependence (linear regression) between bulk density (D_b) and longitudinal wave velocity (V_P) can be seen in Figure 10.

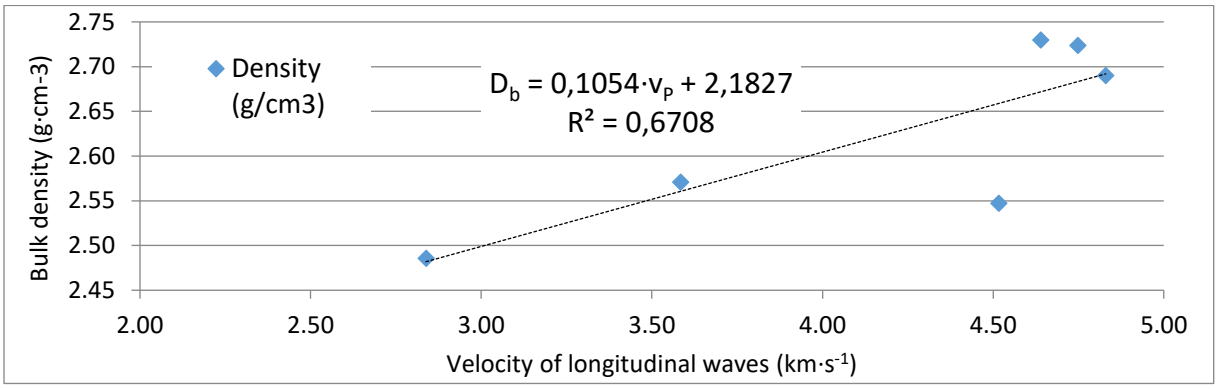

Figure. 10. Dependence (linear regression) between bulk density (D_b) and longitudinal wave velocity (V_P)

It can be seen in Figure 10 that there is a linear regression relationship between bulk density and longitudinal wave velocity with a satisfactory R^2 reliability value.

It is assumed that permeability increases with increasing porosity. The relationship (linear regression) between porosity (Por) and permeability (Per) can be seen in Figure 11.

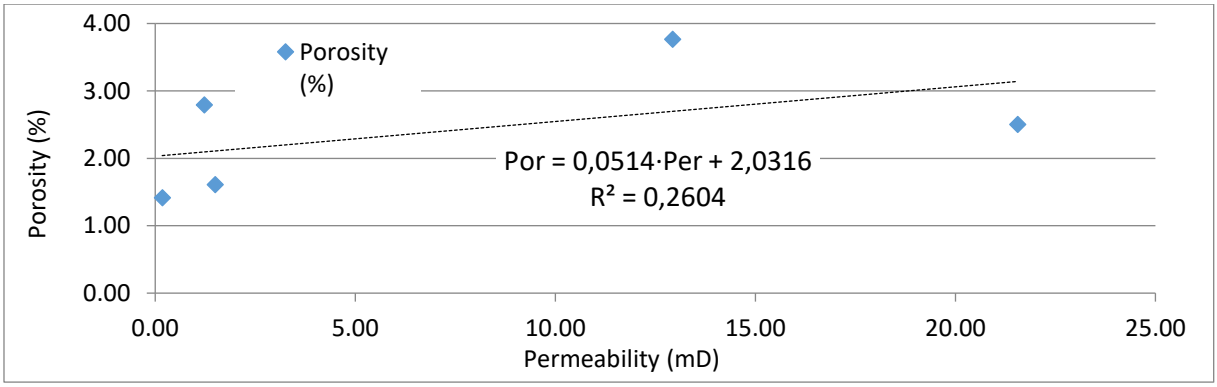

Figure. 11. Relationship (linear regression) between porosity (Por) and permeability (Per)

It can be seen in Figure 11 that the assumption of increasing bulk density with decreasing porosity was only partially confirmed. Low-reliability value is recorded.

Furthermore, it can be concluded that as the pore compressibility increases, the volume compressibility increases. It can also be assumed that the value of the Biott coefficient increases with increasing pore and volume compressibility. The dependence (linear regression) between pore (C_{pc}) and volume compressibility (C_{bc}), further between pore compressibility and the value of the Biott coefficient (BiC) and likewise between the volume compressibility and the value of the Biott coefficient can be seen from Figure 12.

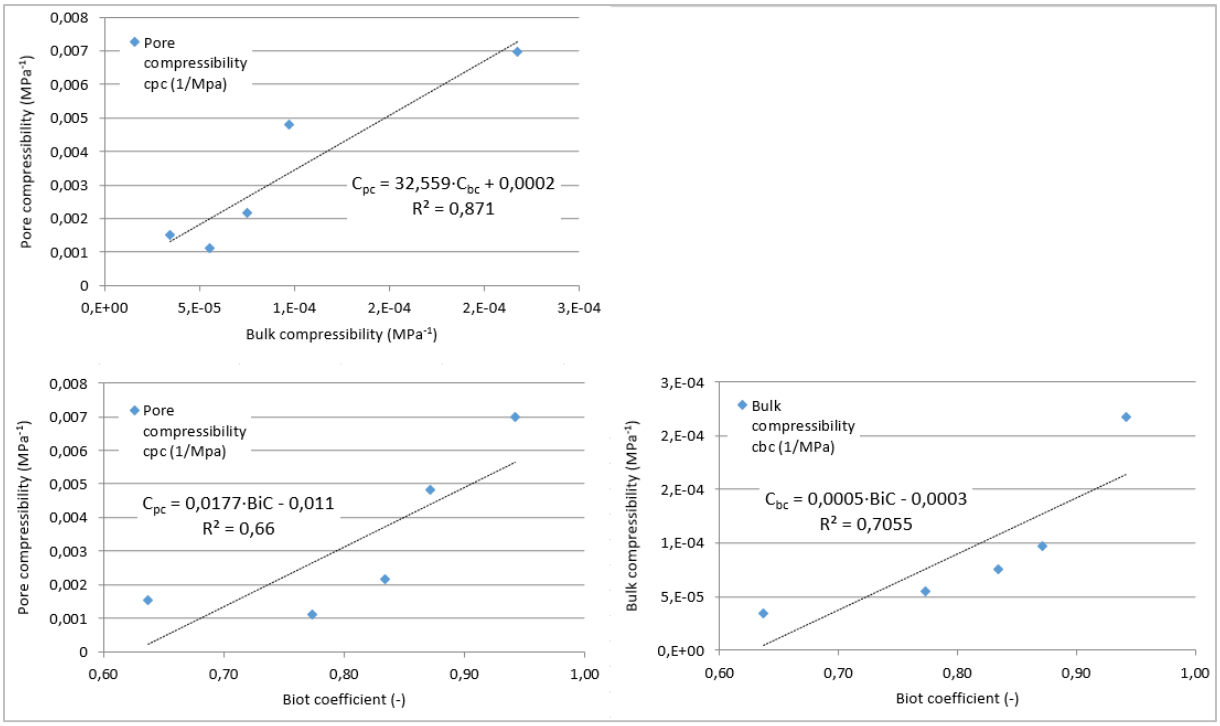

Figure. 12. Dependence (linear regression) between pore (PoC) and volume compressibility (BuC), between pore compressibility and the value of the Biott coefficient (BiC), and between the volume compressibility and the value of the Biott coefficient

It can be seen from Figure 12 that the stated assumptions were generally confirmed by the research works. A satisfactory R^2 reliability value is recorded.

Dependence (linear regression) between unconfined compressive strength (UCS) and pore strength (C_{pc}), resp. volume compressibility (C_{bc}) can be seen in Figure 13.

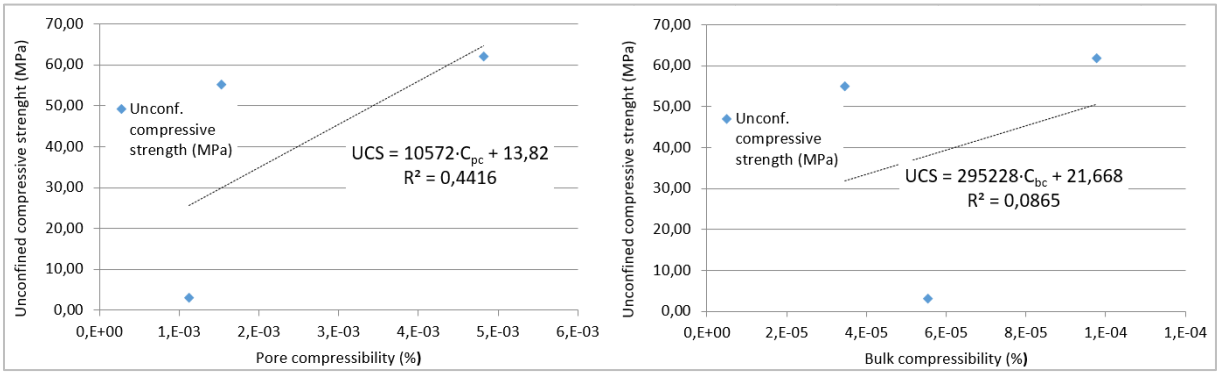

Figure. 13. Dependence between simple compressive strength (UCS) and pore strength (C_{pc}), resp. volume compressibility (C_{bc})

Porosity significantly affects rock strength. With increasing porosity, the speed of propagation of elastic waves should decrease, and thus the mechanical-elastic characteristics. The presence of pores in the rock creates a kind of barrier that slows down the passing waves. [29] Dependence (linear regression) between porosity (Por) and transverse wave propagation velocity (V_S), longitudinal wave propagation velocity (V_P), dynamic modulus of elasticity (E_dyn) and dynamic shear modulus of elasticity (G_dyn) can be seen in Figure 14.

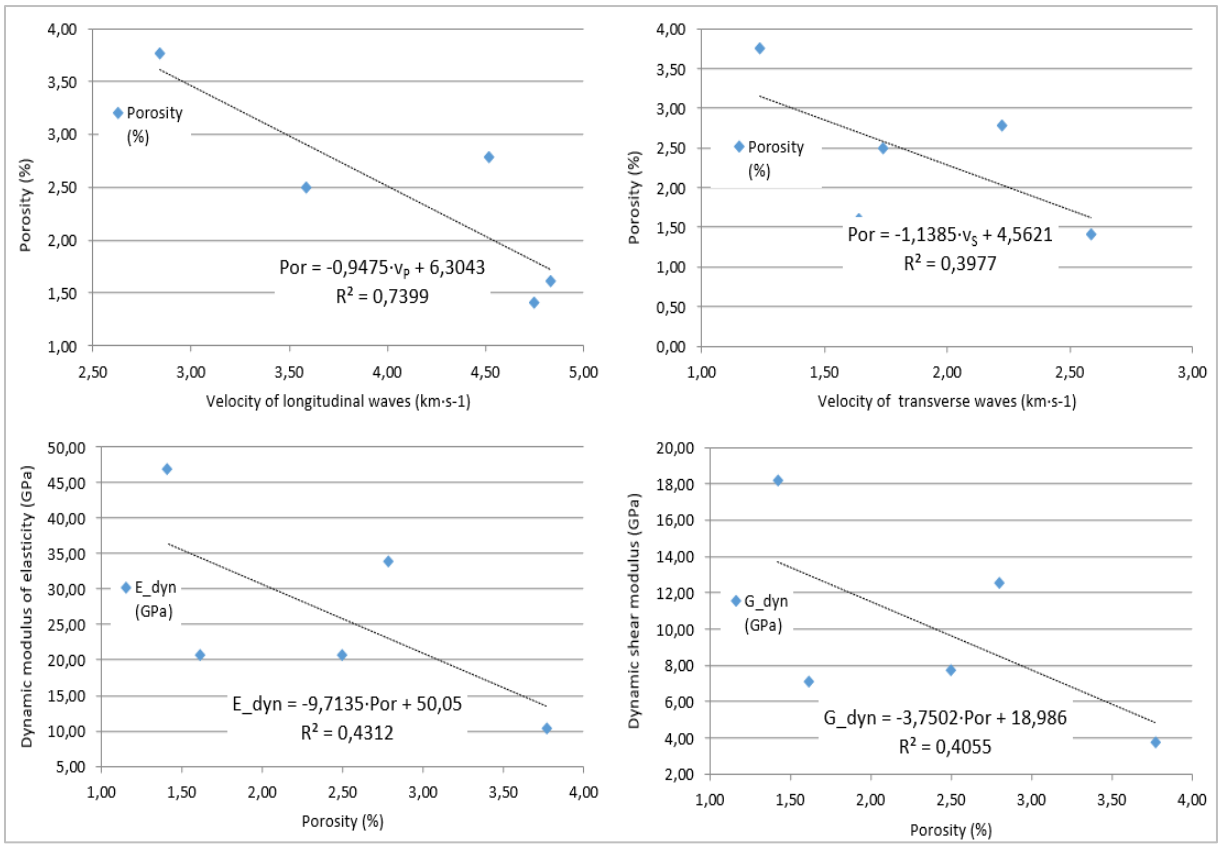

Figure. 14. Dependence (linear regression) between porosity (Por) and velocity of transverse waves (V_S), velocity of longitudinal waves (V_P), dynamic modulus of elasticity (E_dyn) and dynamic modulus of elasticity in shear (G_dyn)

It can be seen in Figure 14 that the assumption of a decreasing speed of propagation of elastic waves and mechanical-elastic characteristics with increasing porosity was basically confirmed. Satisfactory values of reliability R^2 are achieved as a function of linear regression of transverse wave propagation velocity (V_S) and porosity.

Different porosity was demonstrated. On the basis of the obtained data, it can be concluded that the factor of different porosity affects the propagation speed of elastic waves, and therefore also the elastic-mechanical parameters.

1.10. The factor of different degree of saturation

It can be assumed that the different degree of saturation affects the propagation speed of elastic waves. In many research studies, it is reported that as the degree of rock saturation (for samples with approximately the same porosity) increases, the propagation speed of elastic waves also increases [19, 30-33].

Determining the degree of saturation was not the subject of the research.

1.11. Anisotropy factor of rock samples

Rocks, as natural materials, are characterized by a certain anisotropy. Different structural and textural arrangements of rock samples can affect the propagation speed of elastic waves [34].

The determination of anisotropy of rock samples was not the subject of research.

2. Discussion

Although rocks of the same petrographic type, taken from one deposit of the same reservoir structure, were tested as part of the research, relatively significant differences in the observed mechanical-elastic parameters are recorded. It was an effort to determine whether there is a dependence between mechanical-elastic parameters and other observed parameters of petrophysical and mechanical properties.

From the results presented, it is evident that there is a dependence in the form of linear regression for some monitored parameters. This is particularly the case with the dependence between porosity and the propagation speed of longitudinal waves, or volume mass and velocity of propagation of longitudinal waves. The respective graphs show the equations of linear regression in the form of a straight line, i.e. $y = k \cdot x + b$. The straight line k indicates the steepness of the straight line, i.e. how intensively the value of one parameter (longitudinal wave speed) decreases/increases on the other observed parameter (porosity, volumetric mass).

Linear regression equations of the dependence of porosity and velocity of propagation of longitudinal waves, obtained both by current and archival research (research of carbonate rocks), are presented in Table 2. Values of the slope k are graphically highlighted according to this scheme:

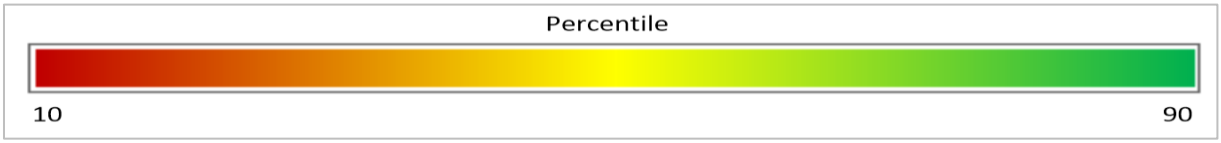

Table 2. Dependence (linear regression) between porosity (Por) and velocity of longitudinal waves (V_P)

Linear regression	Value of reliability R^2	Guideline k	Archival research
Por = -0,8475·v_P + 6,3043	0,7399	-0,8475	Presented research
Por = -6,348·v_P + 37,984		-6,348	Sayed et al., 2015
Por = -6,33·v_P + 39,293		-6,33	
Por = -4,733·v_P + 29,377	0,884	-4,733	Kahraman and Yeken, 2008
Por = -11,236·v_P + 59,7416	0,46	-11,236	Assefa et al., 2003
Por = - 1,899·v_P + 15,24	0,74	-1,899	Pappalardo, 2015
Por = -0,719·v_P + 6,377	0,6	-0,719	Pappalardo, 2015
Por = -4·v_P + 3,1465	0,85	-4	Kurtulus et al., 2016

It can be seen from Table 2 that the presented research found a smaller angle of the guideline than what was found by archival research. However, it should be mentioned that the presented research examined samples with a low porosity range (1 to 4%).

Linear regression equations of the dependence of porosity and velocity of propagation of longitudinal waves, obtained both by current and archival research (research of carbonate rocks), are presented in Table 3. Values of the slope k are graphically highlighted according to this scheme:

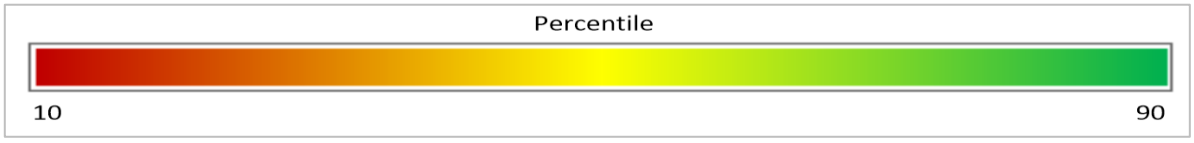

Table 3. Dependence (linear regression) between bulk density (D_b) and velocity of longitudinal waves (V_P)

Linear regression	Value of reliability R^2	Guideline k	Archival research
$D_b = 0{,}1054 \cdot v_P + 2{,}1827$	0,9708	0,1054	Presented research
$D_b = 0{,}27 \cdot v_P + 1{,}13$		0,27	Sayed et al., 2015
$D_b = 0{,}382 \cdot v_P + 0{,}446$		0,382	
$D_b = 0{,}213 \cdot v_P + 1{,}256$	0,821	0,213	Kahraman and Yeken, 2008
$D_b = 0{,}2316 \cdot v_P + 1{,}7384$	0,81	0,2316	Yasar and Erdogan, 2004
$D_b = 0{,}213 \cdot v_P + 1{,}256$	0,821	0,213	Kahraman and Yeken, 2008
$D_b = 0{,}28 \cdot v_P + 1{,}59$	0,934	0,28	Saskar et al., 2012
$D_b = 0{,}3 \cdot v_P + 0{,}9815$	0,8794	0,3	Kurtulus et al., 2016

It can be seen from Table 3 that the presented research found a smaller angle of the guideline than what was found by archival research. However, it should be mentioned that the presented research examined samples with a low porosity range (1 to 4%).

3. Conclusion

As part of the research, geomechanical tests of carbonate rocks were carried out. The samples were taken from the reservoir structure of the Žarošice deposit. Potentially, the possibility of geosequestration of CO_2 into this reservoir structure is being considered. Geosequestration of CO_2 must be preceded by a series of geomechanical tests verifying the petrophysical and mechanical properties of the rocks.

Although carbonate rocks of practically identical mineralogical composition, taken from the same deposit and the same reservoir structure, were tested as part of the research work, relatively significant differences in the propagation speed of elastic waves, and therefore also in the mechanical-elastic characteristics, are recorded. Possible factors that may affect the propagation velocity of elastic waves have been interpreted. Using the values of petrophysical and mechanical properties (possible factors affecting the speed of propagation of elastic waves), it was determined whether there is a dependence between these properties and the speed of propagation of elastic waves. Linear regression relationships (equations) were established between porosity, resp. volume mass and velocity of longitudinal waves.

In the discussion, a comparison of the results of linear regressions of monitored dependencies, determined on the one hand by various authors who have conducted research on carbonate rocks in the past, and on the other hand determined by the presented research is made. The linear regression equations determined by the presented research are quite similar to those determined by other authors. However, it must be said that in the presented research, samples with a low porosity range were observed (approx. 1 to 4%, while other authors studied samples with porosity up to approx. 20%).

4. Acknowledgment

This article was prepared as a part of the CO_2-SPICER project (CO_2 Storage Pilot In a Carbonate Reservoir) - project No:TO01000112, finaced by Technology Agency of the Czech Republic.

References

1. Le Guen, Y., et al., *Enhanced deformation of limestone and sandstone in the presence of high fluids.* Journal of Geophysical Research: Solid Earth, 2007. **112**(B5).
2. Zemke, K., A. Liebscher, and M. Wandrey, *Petrophysical analysis to investigate the effects of carbon dioxide storage in a subsurface saline aquifer at Ketzin, Germany (CO2SINK).* International Journal of Greenhouse Gas Control, 2010. **4**(6): p. 990-999.
3. *Mapy.cz: Base map. [online] 2023. ©Seznam.cz, a.s., ©www.basemap.at, ©Microsoft Corporation, ©OpenStreetMap. Available from: https://mapy.cz/zakladni?source=muni&id=5688&ds=1&x=17.4242715&y=49.0393581&z=6.*
4. Jun, Y.-S., D.E. Giammar, and C.J. Werth, *Impacts of geochemical reactions on geologic carbon sequestration*. 2013, ACS Publications.
5. Gherardi, F., T. Xu, and K. Pruess, *Numerical modeling of self-limiting and self-enhancing caprock alteration induced by CO2 storage in a depleted gas reservoir.* Chemical Geology, 2007. **244**(1-2): p. 103-129.
6. Rohmer, J., A. Pluymakers, and F. Renard, *Mechano-chemical interactions in sedimentary rocks in the context of CO2 storage: Weak acid, weak effects?* Earth-Science Reviews, 2016. **157**: p. 86-110.
7. Verdon, J.P., *Significance for secure CO2 storage of earthquakes induced by fluid injection.* Environmental Research Letters, 2014. **9**(6): p. 064022.
8. Crawshaw, J.P. and E.S. Boek, *Multi-scale imaging and simulation of structure, flow and reactive transport for CO2 storage and EOR in carbonate reservoirs.* Reviews in Mineralogy and Geochemistry, 2013. **77**(1): p. 431-458.
9. Steefel, C.I. and K. Maher, *Fluid-rock interaction: A reactive transport approach.* Reviews in mineralogy and geochemistry, 2009. **70**(1): p. 485-532.
10. Hawkes, C., et al. *Geomechanical factors affecting geological storage of CO2 in depleted oil and gas reservoirs: risks and mechanisms*. in *ARMA North America Rock Mechanics Symposium*. 2004. ARMA.
11. *Hladík V., R. Procházc, P. Jirman (CGS), V. Opletal, M. Pagáč (MND), R. Berenblyum, A. Shchipanov, E. Ford, A. Nermoen (NORCE), June 2021. Presentation of the CO2-SPICER project at the 11th Trondheim CCS conference (TCCS-11).*
12. Kostelnek, P., V. Ciprys, and J. Berka, *Examples of recently discovered oil and gas fields in the Carpathian foredeep and in the European foreland plate underneath the Carpathian thrust belt, Czech Republic.* 2006.
13. ADÁMEK, J., *Geological knowledge about Mesozoic structure of. southeastern slope of the Bohemian Massif section.* Zemní Plyn a Nafta, 1986. **31**(4): p. 453–484.
14. Picha, F.J., Z. Strnk, and O. Krej, *Geology and hydrocarbon resources of the Outer Western Carpathians and their foreland, Czech Republic.* 2006.
15. *Bujok, P.: Influence such as drilling exploration, exploitation and storage of liquid and gaseous hydrocarbon on natural environment. Collection of scientific papers of Faculty of Mining and Geology, VSB – Technical University of Ostrava. Ostrava 2003.*
16. Zayed, E.M., et al., *Development and characterization of AA5083 reinforced with SiC and Al 2 O 3 particles by friction stir processing.* Engineering design applications, 2019: p. 11-26.
17. Krasil'nikov, V., *Sound and ultrasound waves*. 1963: NASA.
18. Kinsler, L.E., et al., *Fundamentals of acoustics*. 2000: John wiley & sons.
19. Kassab, M.A. and A. Weller, *Study on P-wave and S-wave velocity in dry and wet sandstones of Tushka region, Egypt.* Egyptian Journal of Petroleum, 2015. **24**(1): p. 1-11.

20. Sharo, A.A. and M.S. Al-Tawaha, *Prediction of engineering properties of basaltic rocks in Jordan.* International Journal of Civil Engineering and Technology (IJCIET), 2019. **10**(1): p. 1731-1739.
21. Zimmerman, R.W., *Compressibility of sandstones.* 1990.
22. Hall, H.N., *Compressibility of reservoir rocks.* Journal of Petroleum Technology, 1953. **5**(01): p. 17-19.
23. Ahmed, T., *Reservoir engineering handbook 10*. 2010, Gulf Professional Publishing (Elsevier).
24. Ingraham, M.D., et al., *Evolution of permeability and Biot coefficient at high mean stresses in high porosity sandstone.* International Journal of Rock Mechanics and Mining Sciences, 2017. **96**: p. 1-10.
25. Gaviglio, P., *Longitudinal waves propagation in a limestone: the relationship between velocity and density.* Rock Mechanics and Rock Engineering, 1989. **22**(4): p. 299-306.
26. Yasar, E. and Y. Erdogan, *Correlating sound velocity with the density, compressive strength and Young's modulus of carbonate rocks.* International Journal of Rock Mechanics and Mining Sciences, 2004. **41**(5): p. 871-875.
27. Kahraman, S. and T. Yeken, *Determination of physical properties of carbonate rocks from P-wave velocity.* Bulletin of Engineering Geology and the Environment, 2008. **67**: p. 277-281.
28. Kurtulus, C., S. Cakir, and A. Yoğurtcuoğlu, *Ultrasound Study of Limestone Rock Physical and Mechanical Properties.* Soil Mechanics & Foundation Engineering, 2016. **52**(6).
29. Abdelhedi, M., et al., *Ultrasonic velocity as a tool for geotechnical parameters prediction within carbonate rocks aggregates.* Arabian Journal of Geosciences, 2020. **13**: p. 1-11.
30. Kahraman, S., M. Fener, and C.O. Kilic, *Estimating the wet-rock P-wave velocity from the dry-rock P-wave velocity for pyroclastic rocks.* Pure and Applied Geophysics, 2017. **174**: p. 2621-2629.
31. Karakul, H. and R. Ulusay, *Empirical correlations for predicting strength properties of rocks from P-wave velocity under different degrees of saturation.* Rock mechanics and rock engineering, 2013. **46**: p. 981-999.
32. Kahraman, S., *The correlations between the saturated and dry P-wave velocity of rocks.* Ultrasonics, 2007. **46**(4): p. 341-348.
33. Wyllie, M.R.J., A.R. Gregory, and L.W. Gardner, *Elastic wave velocities in heterogeneous and porous media.* Geophysics, 1956. **21**(1): p. 41-70.
34. Garia, S., et al., *A comprehensive analysis on the relationships between elastic wave velocities and petrophysical properties of sedimentary rocks based on laboratory measurements.* Journal of Petroleum Exploration and Production Technology, 2019. **9**: p. 1869-1881.